



HAL
open science

Kirchhoff's generalised law applied to amorphous silicon / crystalline silicon heterostructures

Rudolf Brüggemann

► **To cite this version:**

Rudolf Brüggemann. Kirchhoff's generalised law applied to amorphous silicon / crystalline silicon heterostructures. *Philosophical Magazine*, 2009, 89 (28-30), pp.2519-2529. 10.1080/14786430903074805 . hal-00519092

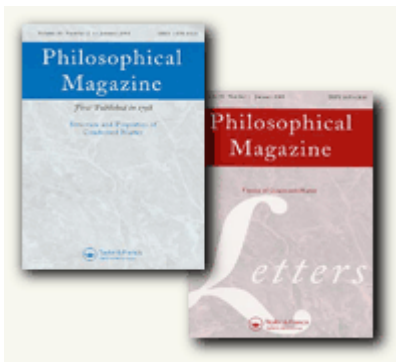
HAL Id: hal-00519092

<https://hal.science/hal-00519092>

Submitted on 18 Sep 2010

HAL is a multi-disciplinary open access archive for the deposit and dissemination of scientific research documents, whether they are published or not. The documents may come from teaching and research institutions in France or abroad, or from public or private research centers.

L'archive ouverte pluridisciplinaire **HAL**, est destinée au dépôt et à la diffusion de documents scientifiques de niveau recherche, publiés ou non, émanant des établissements d'enseignement et de recherche français ou étrangers, des laboratoires publics ou privés.



**Kirchhoff's generalised law applied to amorphous silicon /
crystalline silicon heterostructures**

Journal:	<i>Philosophical Magazine & Philosophical Magazine Letters</i>
Manuscript ID:	TPHM-09-Mar-0135.R1
Journal Selection:	Philosophical Magazine
Date Submitted by the Author:	25-May-2009
Complete List of Authors:	Brüggemann, Rudolf; Carl von Ossietzky Universität Oldenburg, Institut für Physik
Keywords:	electroluminescence, photoluminescence, silicon
Keywords (user supplied):	electroluminescence, photoluminescence, silicon



1
2
3
4
5
6
7
8
9
10
11
12
13
14
15
16
17
18
19
20
21
22
23
24
25
26
27
28
29
30
31
32
33
34
35
36
37
38
39
40
41
42
43
44
45
46
47
48
49
50
51
52
53
54
55
56
57
58
59
60

Kirchhoff's generalised law applied to amorphous silicon / crystalline silicon heterostructures

R. BRÜGGEMANN

Institut für Physik, Carl von Ossietzky Universität Oldenburg, 26111 Oldenburg, Germany

The electro- and photoluminescence spectra of amorphous silicon / crystalline silicon heterostructures and solar cells are determined by emission from the crystalline-silicon layer and are computed with Kirchhoff's generalised law. The interface defect density strongly influences the luminescence yield which may be used to monitor the interface quality. Based on a comparison between numerical and analytically determined spectra, the temperature dependence of experimental electroluminescence and photoluminescence spectra of these silicon heterostructures is analysed. We find a clear indication of the validity of Kirchhoff's generalised law for the luminescence emission from these silicon structures and conclude that it can be applied between 112 K and 363 K without further modification in order to account for the indirect nature of the optical transitions in crystalline silicon.

Keywords: Photoluminescence, Electroluminescence, Silicon

Tel. +49-441-7983481

Fax +49-441-7983201

Email rudi.brueggemann@uni-oldenburg.de

1. Introduction

Since the report by Spear and LeComber [1] on substitutional doping of hydrogenated amorphous silicon (a-Si:H) quite a number of a-Si:H based device types have been developed. Spear's group published a first paper on a fully amorphous-silicon *pn*-junction device [2] and it was concluded that the photovoltaic response was qualitatively similar to a monocrystalline silicon diode. However, because of the short diffusion lengths in the doped amorphous layers, a fully amorphous solar cell requires a pin-type device with an intrinsic amorphous layer with low defect density. In a *pn*-junction solar cell, the amorphous film as the emitter consists only of a doped layer of a few nanometer thickness, deposited on a standard monocrystalline (c-Si) silicon wafer as the absorber with opposite doping. More sophisticated structures involve additional amorphous layers at the front and rear interface of the wafer. These heterojunction silicon solar cells have reached photovoltaic efficiencies in excess of 22% [3]. In this Sanyo HIT solar cell, an intrinsic thin layer is deposited between the wafer and the doped amorphous layer.

The optimisation of these heterostructures depends on a large degree on the control of properties of the interface between the front a-Si:H layers and the c-Si wafer. Here, both the wafer pre-treatment prior to the amorphous silicon deposition and the a-Si:H deposition itself, typically by plasma enhanced chemical vapour deposition (PECVD), are important, e.g. [3-7]. In addition, the back-contact properties have been investigated and improved.

In order to assist in the understanding of the device physics and optimisation, device simulation gives an insight into the device properties. For this reason, simulation programmes have been developed, namely SC-Simul [8,9] and AFORS-HET [10,11] with particular emphasis on the simulation of a-Si:H/c-Si heterojunction solar cells with their thick c-Si layers. For example, the influence of interface defects on the device in the dark and under illumination can be studied. Based on the numerical results, it was shown [12] that the a-

Si:H/c-Si heterostructure based on n-type wafers with holes as minority carriers is less affected by the interface defects than p-type wafer structures, because of the reduced minority-carrier related interface-recombination rate related to the interface-defect charge in the former.

In the present work, we apply numerical modelling to investigate the analytical description for luminescence emission from these structures. We relate the electroluminescence efficiency to the interface quality. We re-examine recent findings of the mismatch between experimental electroluminescence spectra and Kirchhoff's generalised law [15]. Here, we demonstrate that Kirchhoff's generalised law [13,14] can be applied to describe the luminescent photon flux from these amorphous silicon / crystalline silicon heterostructures without modifications.

2. Theory

According to Stern and Lasher [16], the spontaneous band-to-band radiative recombination rate per energy interval for recombination between conduction-band electrons and valence-band holes is given by

$$dr_{spont}(\hbar\omega) = \frac{n_r^2(\hbar\omega)^2}{\pi^2 \hbar^3 c_0^2} \frac{\alpha(\hbar\omega) d\hbar\omega}{\exp\left(\frac{\hbar\omega - (\varepsilon_{Fn} - \varepsilon_{Fp})}{kT}\right) - 1} \quad (1)$$

where n_r is the refractive index, c_0 the vacuum light velocity, α is the absorption coefficient, k is the Boltzmann constant, T is the temperature and the quasi-Fermi levels of the conduction-band electrons and the valence-band holes are ε_{Fn} and ε_{Fp} . The emitted photon flux density into one hemisphere can then be described by this quasi-Fermi level splitting, $\varepsilon_{Fn} - \varepsilon_{Fp}$, and the absorptivity A of the sample by [13]

$$dj_\gamma(\hbar\omega) = \frac{(\hbar\omega)^2}{4\pi^2 \hbar^3 c_0^2} A(\hbar\omega) \exp\left(-\frac{\hbar\omega}{kT}\right) \exp\left(\frac{\varepsilon_{Fn} - \varepsilon_{Fp}}{kT}\right) d(\hbar\omega), \quad (2)$$

where the “-1” in the Bose-term has been neglected.

For a symmetrical wafer A is given by

$$A(\hbar\omega) = \frac{(1 - R_{int}(\hbar\omega))(1 - e^{-\alpha(\hbar\omega)d})}{1 - R_{int}(\hbar\omega)e^{-\alpha(\hbar\omega)d}}. \quad (3)$$

with the reflection coefficient of the air/wafer interface, R_{int} and the sample thickness d . Multiple reflections are taken into account here.

In Eq. (2), the assumption has been made that $\varepsilon_{Fn} - \varepsilon_{Fp}$ is spatially constant across the wafer. The spectral shape of the emitted radiation is thus mainly determined by the product of the energy-dependent Boltzmann term and the absorptivity of the sample structure under study. The height of the spectrum is scaled by the exponential dependence on $\varepsilon_{Fn} - \varepsilon_{Fp}$, which reflects the product of the free electron and hole densities, together with the intrinsic carrier density and kT term.

The term for A is modified for a solar cell with a rear-side mirror-like contact. With the nominally photon-energy dependent front-reflection coefficient R_f and the back-reflection coefficient R_b the absorptivity reads

$$A(\hbar\omega) = \frac{(1 - R_f) \left[(1 - R_b)e^{-2\alpha d} - (1 - R_b)e^{-\alpha d} \right]}{1 - R_f R_b e^{-2\alpha d}}. \quad (4)$$

For non-homogeneous carrier distributions and thus a non-constant quasi-Fermi level splitting, a more complicated version of Eq. (2) involves an integral term to take into account the non-homogeneous generation and propagation of the luminescence photons. For emission through the front interface at $z = d$ and the rear interface at $z = 0$ the photon current density into the hemisphere reads

$$dj_\gamma(\hbar\omega) = \frac{(\hbar\omega)^2}{4\pi^2 \hbar^3 c_0^2} \frac{\alpha(\hbar\omega)(1 - R_f) \exp[-\alpha(\hbar\omega)d]}{1 - R_f R_b \exp[-2\alpha(\hbar\omega)d]} \int_0^d \left[\exp(\alpha(\hbar\omega)z) + R_b \exp(-\alpha(\hbar\omega)z) \right] \exp\left(-\frac{\hbar\omega}{kT}\right) \exp\left(\frac{\varepsilon_{Fn}(z) - \varepsilon_{Fp}(z)}{kT}\right) dz \quad d(\hbar\omega) \quad (5)$$

where again the “-1” in the Bose-term has been neglected.

Eq. (2) can be related to the emitted electroluminescence (EL) radiation of a solar cell at an applied voltage V_a . Würfel [14] pointed out that for a luminescent pn diode at forward bias, with the quasi-Fermi level splitting being almost constant in space, $\varepsilon_{Fn} - \varepsilon_{Fp}$ in the whole volume equals eV_a , and thus from Eq. (2) it follows that

$$d j_y(\hbar\omega) = \frac{(\hbar\omega)^2}{4\pi^2\hbar^3c_0^2} A(\hbar\omega) \exp\left(-\frac{\hbar\omega}{kT}\right) \exp\left(\frac{V_a}{kT}\right) d(\hbar\omega). \quad (6)$$

The emitted photon flux thus depends exponentially on the applied voltage if no series resistance applies and scales linearly with the current in a Shockley diode.

For the photoluminescence experiment, Eqs. (2) or (5) may also be applied. Here the splitting of the quasi-Fermi levels is also determined by the local photogeneration rate together with the transport properties of the excess carriers and $\varepsilon_{Fn} - \varepsilon_{Fp}$ is almost constant for long diffusion lengths with respect to absorber thickness.

3. Simulation

The simulation software SC-Simul [5,6] solves the transport equations and Poisson's equation and allows the device modelling of heterojunction solar cells with different layers. The programme determines all the physical properties of interest, e.g., the quasi-Fermi levels or the free electron and hole densities, the electrostatic potential and other properties like recombination rates. The input parameters are the semiconductor properties of the different layers with which a structure is built, like the band gap E_g , effective densities of states in the band, free carrier mobilities, electron affinity, capture coefficients for defect states and parameters for defect densities and distributions. Eq. (5) is applied to calculate the luminescence spectrum from the numerical solution of the device equations.

4. Experimental details

In the electroluminescence experiment, the luminescent radiation from the solar cell, driven by a Keithley 2400 sourcemeter, is collected and dispersed by a monochromator and measured by a liquid-nitrogen cooled InGaAs diode. For photoluminescence experiments the sample is illuminated with a laser of suitable photon energy. The setup is calibrated with a tungsten band lamp for determining absolute photon fluxes.

5. Simulation

5.1 Results

Figure 1 shows simulation results of the electroluminescence spectra of a 300 μm thick heterojunction (n)a-Si:H/(p)c-Si solar cell with 5 nm a-Si:H layer at a current density of 111 mA cm^{-2} at an applied voltage of 0.74 V. For simplicity, the values for R_f and R_b are 0 and 1. The electron diffusion length is 815 μm , exceeding the thickness. The complete description with Eq. (5) is applied to the numerical solution of the quasi-Fermi level splitting to calculate the spectrum, given by the symbols. The analytical solution of Eq. (6) is given by a full line, i.e. it is calculated under the assumption of constant quasi-Fermi level splitting. The additional line gives the spectrum according to [17] for the case of no re-absorption if the absorption coefficient α instead of the absorption A is used, which is, because of the back-reflection, adjusted here for the low-energy data where A is $2\alpha d$.

Fig. 2 shows the analytical electroluminescence spectra at 0.74 V of the 300 μm thick cell of Fig. 1 and the cell with the same parameters but 70 μm thickness. As the high energy wing is determined by the absorption, the spectra become identical for photon energies at about > 1.3 eV at which A saturates also for the thin sample.

Fig. 3 compares the analytical photoluminescence spectra of a wafer and of the cell of Fig. 1 for the same quasi-Fermi level splitting, respectively $\varepsilon_{Fn} - \varepsilon_{Fp} = e V_a$. The dashed line is

1
2
3 calculated with Eqs. (2) and (3) with a symmetrical structure and $R_{int} = 0$. The high-energy
4 wing is identical while the wafer shows lower emitted photon flux for photon energies < 1.2
5 eV. The dotted line is the shifted dashed line for adjustment of the wafer and cell spectra at
6 the maximum position.
7
8
9
10
11

12 The increase in the interface defect density N_{if} results in a decrease in the
13 electroluminescence emission output of the heterojunction cell. Fig. 4 shows this decrease for
14 two solar cells where the spectra have been numerically calculated with SC-Simul at the same
15 current density of 111 mA cm^{-2} . The drop in the EL quantum efficiency, defined by the ratio
16 of emitted photon per flowing electron, $e \Phi / j$, is about a factor of 23, where the integral of
17 the spectra has been evaluated. In additional evaluations, the open-circuit voltages V_{oc} have
18 been determined with the higher N_{if} resulting in a drop of V_{oc} .
19
20
21
22
23
24
25
26
27
28
29
30
31
32

33 5.2 Discussion

34 The full solution for the spectrum in Fig. 1, based on the numerical solution by SC-Simul
35 and Eq. (5), shows almost perfect agreement with the simple analytical form of Eq. (2). The
36 shape of the spectrum, assigned to the c-Si absorber, is an image of the absorption coefficient
37 in the low-energy range where $A \propto \alpha$. In the high-energy range the slope is related to $(kT)^{-1}$
38 (apart from the $(\hbar\omega)^2$ term) as A becomes $1 - R_f$. If α only and not A is used for the
39 calculation of the spectrum, the discrepancy at high photon energies is obvious. The
40 calculated photon flux here is too high because reabsorption is neglected.
41
42
43
44
45
46
47
48
49
50
51

52 Fig. 2 illustrates that only the high-energy range can be easily used for the determination of
53 the quasi-Fermi level splittings of the luminescence spectra because the energetic variation of
54 A depends on the sample thickness and the absorption coefficient. For the thin sample the
55 slope is related to $(kT)^{-1}$ at about 1.3 eV and higher which indicates the saturation of A .
56
57
58
59
60

1
2
3 The overall emission output is larger for the 300 μm sample but the enhancement is less
4 than the volume factor because of the reabsorption of the high-energy photons, generated in
5 the deeper regions of the cell. Photon recycling in c-Si is negligible so that the simulated
6 spectra are close together in this energy range.
7
8
9
10
11

12 Fig. 3 shows that photoluminescence and electroluminescence output can be comparable as
13 both depend on the quasi-Fermi level splitting which has been taken the same for the two
14 structures, connected by the applied voltage. For the symmetrical structure, photons in the low
15 energy part are missing because they are emitted to the other side of the wafer that does not
16 face the detector. Matching the maxima of the EL and PL spectra results in a mismatch at
17 higher photon energies.
18
19
20
21
22
23
24
25
26

27 Fig. 4 shows the strong influence of increasing N_{if} on the electroluminescence output of the
28 heterojunction cell. A drop in the EL efficiency is easily achieved with increasing N_{if} . This
29 decrease is complementary to the decrease in the open-circuit voltage with increasing N_{if} [17]
30 and the present computations show that it is also related to the increase in dark-saturation
31 current with increasing N_{if} . The ratio in dark-saturation currents is the same as the ratio of the
32 EL efficiencies and also related to $\exp[\Delta V_{oc}/(kT)]$, where ΔV_{oc} is the difference in the two V_{oc} .
33
34
35
36
37
38
39
40
41
42
43
44

45 6. Experiment

46 6.1 Results

47 Fig. 5 shows experimental results of the photoluminescence spectra for different
48 temperatures from a symmetrical c-Si wafer structure passivated with a-Si:H layers. The
49 experimental data have been compared with the analytical presentation of Eq. (2) with a
50 suitable value of R_{int} from an reflection experiment. The analytical expression can be plotted
51 for a limited energy range, respectively, because the optical absorption coefficient is not
52 available for wider ranges.
53
54
55
56
57
58
59
60

1
2
3 Fig. 6 shows temperature-dependent experimental electroluminescence spectra of a
4 heterojunction test cell [19]. The experimental spectra have been compared with the analytical
5 presentation of Eq. (6) in the energy ranges for which the optical absorption coefficient from
6 transmission and reflection measurements was available.
7
8
9
10
11

12 13 14 15 16 **6.2 Discussion**

17
18 The results in Figs. 5 and 6 are a demonstration that Kirchhoff's generalised law is valid
19 for the emission from the c-Si absorber of these amorphous silicon / crystalline silicon
20 heterostructures, for which the a-Si:H layers are so thin that they do not contribute to the
21 signal and for which the photo- and electroluminescence results reflect the optoelectronic
22 properties of the c-Si absorber layer. In the figures, the spectral shape in the high energy range
23 is well reproduced for temperatures between 363 K and 112 K. In the high-energy range the
24 spectra become steeper with decreasing temperature – as it should be according to Eq. (2). In
25 the low energy-range the steeper absorption coefficient – known from optical experiments –
26 results in a steeper spectrum so that the spectra become narrower with decreasing
27 temperature.
28
29
30
31
32
33
34
35
36
37
38
39
40
41

42 Our good agreement between Kirchhoff's generalised law to describe the experimental
43 spectra, which represent the luminescence of c-Si, is in agreement with the findings in [14]
44 but in contrast to a recent report in the literature [15], in which the experimental
45 electroluminescence spectra from a-Si:H/c-Si solar cells were compared with the spectra from
46 the numerical simulation with AFORS-HET, indicating too high values for the simulated
47 spectra in the high-energy range [15], similar to the dashed curve in Fig. 1. Inspection and
48 computation showed [21] that the digitised room-temperature experimental spectra of [15] can
49 be matched with the analytical description of Kirchhoff's generalised law outlined above. In
50 contrast to the conclusions in [15], our fits indicated that no modification was necessary to
51 take extra account of the indirect nature of the optical transitions in crystalline silicon. It is
52
53
54
55
56
57
58
59
60

1
2
3 pointed out that for shorter diffusion lengths and inhomogeneous carrier profiles the simple
4 relations of Eqs. (2) or (6) do not longer hold. Then the spectral shape is also an image of
5 these profiles and may be used for further analysis and evaluation [22].
6
7
8
9

10 11 12 13 14 15 **7. Conclusion**

16
17
18 The comparison of the full numerical solution for the electroluminescence spectrum with
19 an analytical form under the assumption of constant quasi-Fermi level splitting shows good
20 agreement so that our analysis of electroluminescence spectra confirms the simplification by
21 assuming that $\varepsilon_{Fn} - \varepsilon_{Fp}$ equals eV_a . The details of the spectral shape are determined by the
22 optical interface properties and the thickness-dependent absorption properties of the structure.
23
24

25
26
27 The experimental results for the luminescence spectra of c-Si show good agreement with
28 the spectral shape that is determined analytically from Kirchhoff's generalised law under the
29 assumption of constant quasi-Fermi level splitting. This agreement holds also, notably for the
30 high-energy wings of the c-Si emission spectra, for different temperatures in the range
31 between 112 K and 363 K. We thus report good agreement with Kirchhoff's generalised law
32 for this temperature range, applied to amorphous silicon / crystalline silicon heterostructures,
33 and we cannot reproduce the mismatch, reported in [15] for similar structures, between
34 experimental spectra and those from Kirchhoff's generalised law.
35
36
37
38
39
40
41
42
43
44
45
46
47
48
49
50

51 **Acknowledgement**

52
53
54 The author is grateful to the late Walter E. Spear for introducing him into the physics of
55 amorphous semiconductors while studying an MSc course during the academic year 1987/88.
56 The provision of samples from colleagues at ISE Gelsenkirchen and HMI Berlin is gratefully
57 acknowledged. The author thanks S. Meier and J. Behrends for measurements during their
58 thesis projects.
59
60

References

1. W.E. Spear, P.G. LeComber, *Solid State Comm.* **17**, 1193 (1975).
2. W.E. Spear, P.G. LeComber, S. Kinmond, M.H. Brodsky, *Appl. Phys. Lett.* **28**, 105 (1976).
3. Y. Tsunomura M. Taguchia, T. Babaa, T. Kinoshitaa, H. Kannoa, H. Sakataa, E. Maruyamaa, M. Tanaka, *Solar En. Mat. Solar Cells* (2008), doi:10.1016/j.solmat.2008.02.037, in press.
4. K. v. Maydell, H. Windgassen, W. A. Nositschka, U. Rau, P. J. Rostan, J. Henze, J. Schmidt, M. Scherff, W. Fahrner, D. Borchert, S. Tardon, R. Brüggemann, H. Stiebig, M. Schmidt European Photovoltaic Solar Energy Conference, September 2005, Barcelona, Spain, eds.: W. Palz, H. Ossenbrink , P. Helm (WIP, Munich 2005) p. 822.
5. P.-J. Ribeyron, A. Vandeneynde, J. Damon-Lacoste, D. Eon, P. Roca i Cabarrocas, R. Chouffot, J.-P. Kleider, R. Brüggemann, *Proc. 22nd European Photovoltaic Solar Energy Conference, September 2007, Milan, Italy, (WIP, Munich, 2007)* p. 1197.
6. H. M. Branz, C. W. Teplin, D. L. Young, M. R. Page, E. Iwaniczko, L. Roybal, R. Bauer, A. H. Mahan, Y. Xu, P. Stradins, T. Wang, Q. Wang, *Thin Solid Films* **516**, 743 (2008).
7. S. Olibet, E. Vallat-Sauvain, C. Ballif, L. Korte, L. Fesquet, *Proceedings of the 17th Workshop on Crystalline Silicon Solar Cells and Modules: Materials and Processes, Vail, Colorado USA, August, 2007*, p. 130.
8. M. Rösch, PhD Thesis (in German), available online at <http://docserver.bis.uni-oldenburg.de/publikationen/dissertation/2003/roeexp03/roeexp03.html>
9. R. Brüggemann, M. Rösch, *J. Optoelectron. Adv. Mater.* **7**, 65 (2005).
10. A. Froitzheim, R. Stangl, M. Kriegel, L. Elstner, W. Fuhs, *Proc. 3rd World Conference on Photovoltaic Energy Conversion, Osaka, Japan, May 2003*, eds. K. Kurokawa, L.L. Kazmerski, B. McNelis, M. Yamaguchi, C. Wronski, W.C. Sinke (Osaka, 2003), p. 279.
11. R. Stangl, A. Froitzheim, M. Kriegel, T. Brammer, S. Kirste, L. Elstner, H. Stiebig, M. Schmidt, W. Fuhs, *Proc. 19th European Photovoltaic Solar Energy Conference, Paris, France, June 2004*, p. 1497.
12. M. Rösch, R. Brüggemann, G. H. Bauer, *2nd World Conference on Photovoltaic Solar Energy Conversion, Vienna*, eds.: J. Schmid, H.A. Ossenbrink, P. Helm, H. Ehmman, E.D. Dunlop, Joint Research Centre, Ispra, 1998, p. 946.
13. P. Würfel, *J. Phys. C* **15**, 3967 (1982).
14. T. Trupke, E. Daub, P. Würfel, *Solar Energy Materials Solar Cells* **53**, 103 (1998).

- 1
 - 2
 - 3
 - 4
 - 5
 - 6
 - 7
 - 8
 - 9
 - 10
 - 11
 - 12
 - 13
 - 14
 - 15
 - 16
 - 17
 - 18
 - 19
 - 20
 - 21
 - 22
 - 23
 - 24
 - 25
 - 26
 - 27
 - 28
 - 29
 - 30
 - 31
 - 32
 - 33
 - 34
 - 35
 - 36
 - 37
 - 38
 - 39
 - 40
 - 41
 - 42
 - 43
 - 44
 - 45
 - 46
 - 47
 - 48
 - 49
 - 50
 - 51
 - 52
 - 53
 - 54
 - 55
 - 56
 - 57
 - 58
 - 59
 - 60
15. W. Fuhs, A. Laades, K. von Maydell, R. Stangl, O.B. Gusev, E. Terukov, S. Kazitsyna-Baranovski, G. Weiser, *J. Non-Cryst. Solids* **352**, 1884 (2006).
16. G. Lasher, F. Stern, *Phys. Rev.* **133**, A553 (1964).
17. G.H. Bauer, P. Würfel, in *Organic photovoltaics*, eds.: C.J. Brabec; V. Dyakonov; J. Parisi (Springer, Berlin, 2003), pp. 118 - 158.
18. S. Tardon, M. Rösch, R. Brüggemann, T. Unold, G.H. Bauer, *J. Non-Cryst. Solids* **338&340**, 444 (2004).
19. J. Behrends, Diploma thesis, Universität Oldenburg (2006).
20. S. Meier, Diploma thesis, Universität Oldenburg (2006).
21. R. Brüggemann, unpublished.
22. P. Würfel, T. Trupke, T. Puzzer, E. Schäffer, W. Warta, S. Glunz, *J. Appl. Phys.* **101**, 123110 (2007).

Captions

Fig. 1: Electroluminescence spectrum of a 300 μm thick a-Si:H/c-Si solar cell at a current density of 111 mA cm^{-2} and an applied voltage of 0.74 V. The values for R_f and R_b are 0 and 1. The symbols show the result of the computer experiment in which the spectrum is calculated from the nominally spatially dependent electron and hole distributions with Eq. (5). The overlapping full line shows the analytical spectrum according to Eq. (6). The dashed line gives the spectrum if the absorption coefficient α instead of the absorption A is used (adjusted for the low-energy data because A is $2\alpha d$). Then, in the high-energy range the emission is too large because reabsorption is neglected. The slope is then no longer related to $(kT)^{-1}$.

Fig. 2: Analytical electroluminescence spectrum with Eq. (6) of a 70 μm and 300 μm thick a-Si:H/c-Si solar cell at a current density of 111 mA cm^{-2} and an applied voltage of 0.74 V. The latter is identical with that of Fig. 1. The values for R_f and R_b are 0 and 1. There is only an increased output in the low-energy range due to the larger volume and because of the reabsorption of the emitted luminescence photons at higher energies.

Fig. 3: Analytical photoluminescence spectrum of a 300 μm thick c-Si wafer with $R_{int} = 0$ and a quasi-Fermi level splitting of 0.74 eV (dashed line) and electroluminescence spectrum of the 300 μm cell of Fig. 1 (applied voltage of 0.74 V). The dotted line results from shifting the dashed line for adjusting the maxima of the spectra. The PL spectrum of the cell would be identical to the EL spectrum if the quasi-Fermi level splittings were the same.

Fig. 4: Decrease of the emitted photon flux with the higher interface-defect density N_{if} . For the same current a higher voltage V_a must be applied. In a different computer experiment the corresponding open-circuit voltage under AM1.5 illumination also drops.

Fig. 5: Temperature-dependent experimental photoluminescence of a polished c-Si wafer, passivated on both sides by a thin a-Si:H layer. The full lines are representations of the spectra, calculated with Eq. (2) and constant quasi-Fermi level splitting. The temperature-dependent absorption coefficient determines A at the different temperatures, after [19].

Fig. 6: Temperature-dependent experimental electroluminescence of an a-Si:H/c-Si solar cell. The full lines are representations of the spectra, calculated with Eq. (6). The data are more noisy because of the smaller emitted photon flux, after [20].

Figure 1

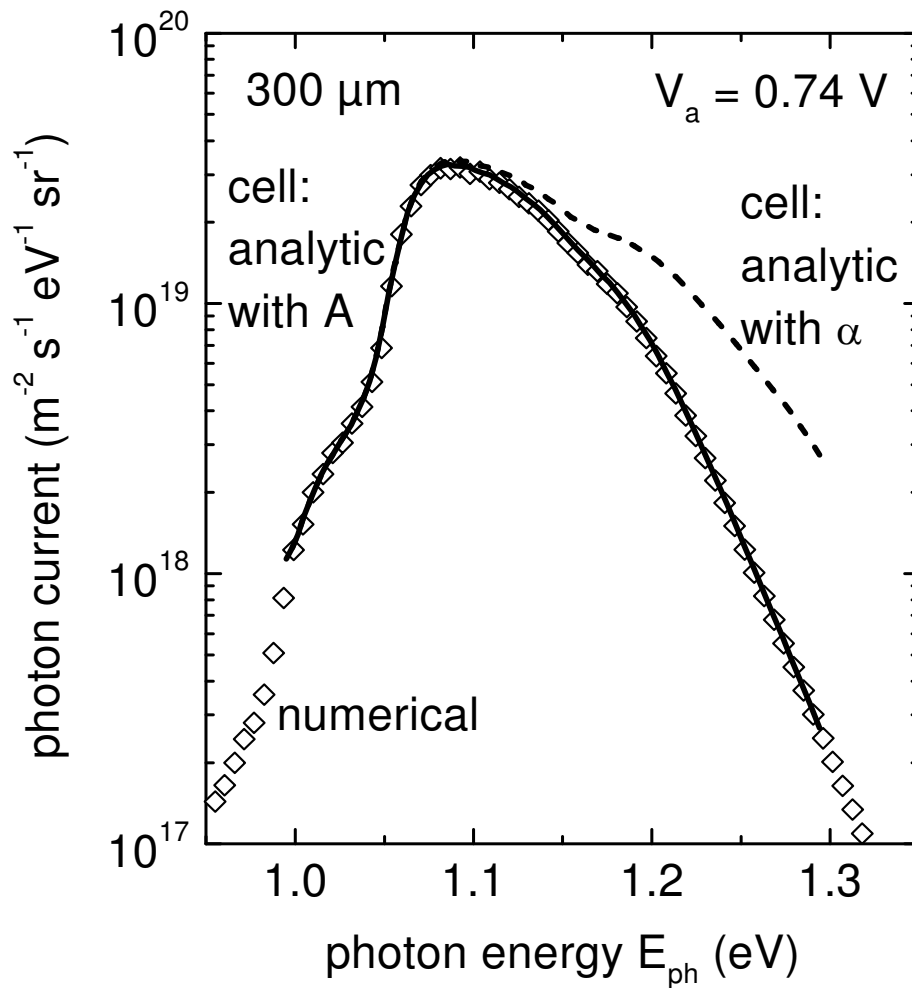


Figure 2

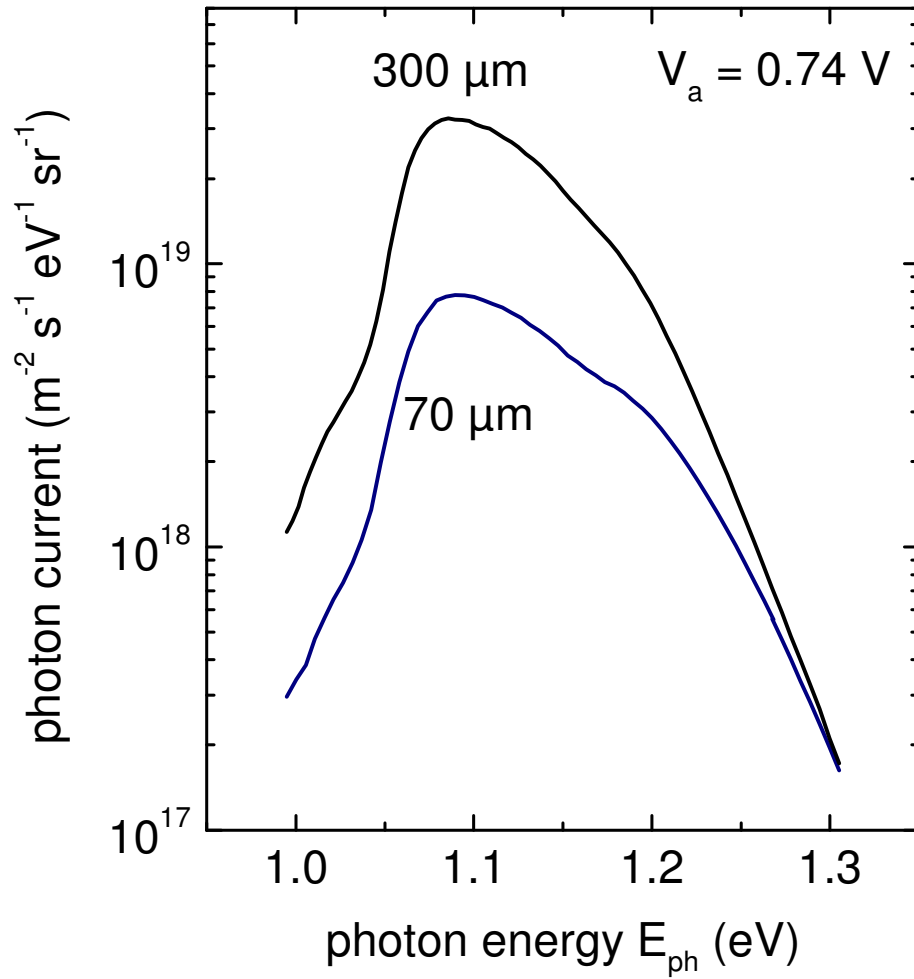


Figure 3

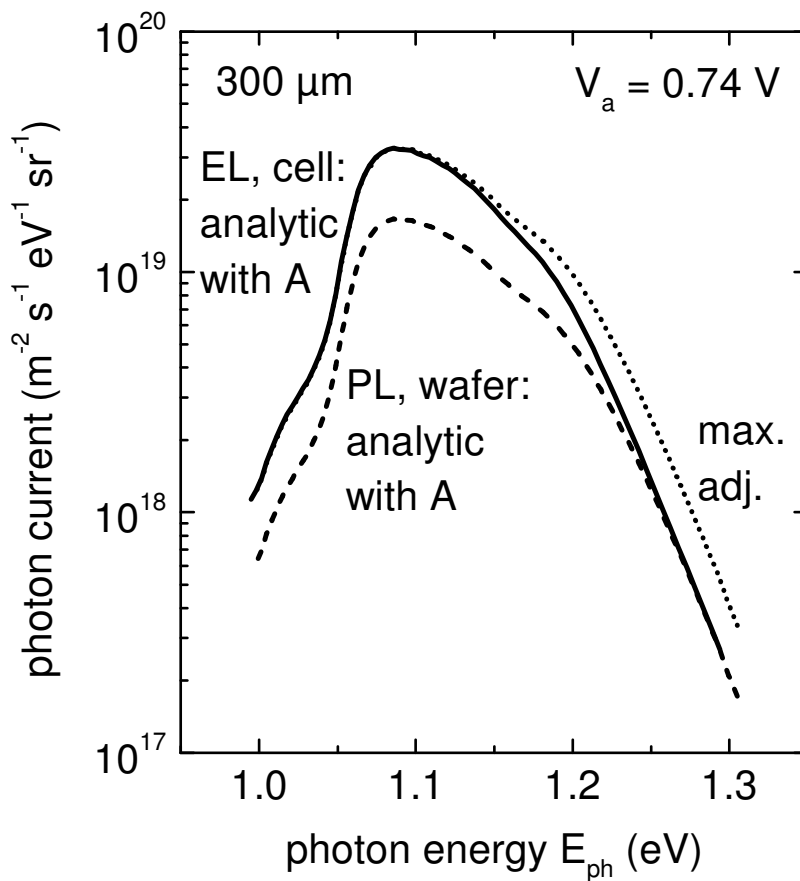


Figure 4

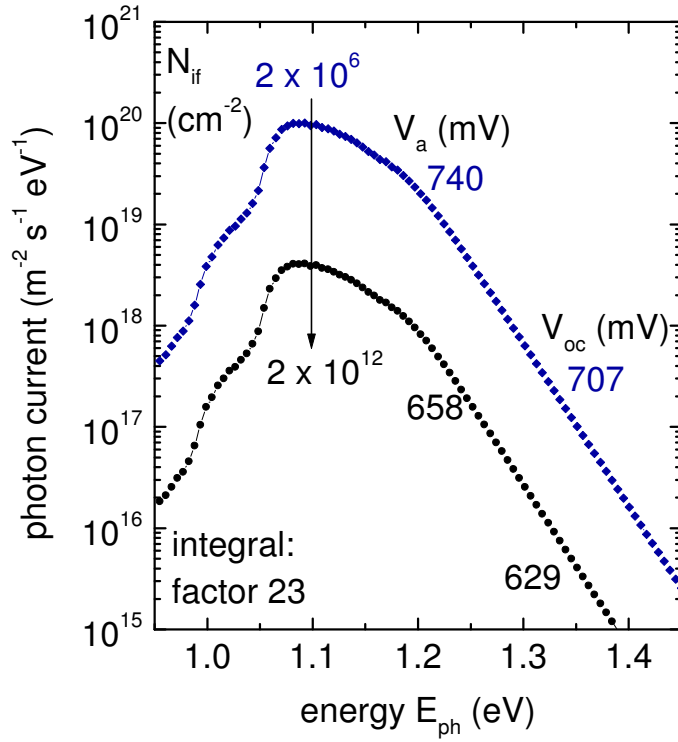


Figure 5

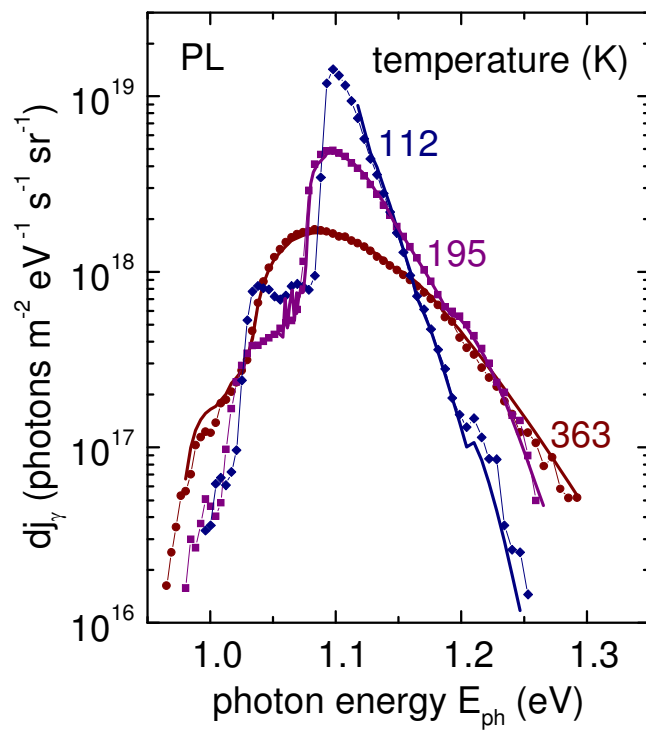


Figure 6

